Available online at www.sciencedirect.com
SCIENCE DIRECT®
Biochemical and Biophysical Research Communications 331 (2005) 370–374
BBRC
www.elsevier.com/locate/ybbrc

Rotary torque produced by proton motive force in FoF_1 motor ☆

Zhang Yinghao [a,c], Wang Jun [b,c], Cui Yuanbo [a,c], Yue Jiachang [a,*], Fang Xiaohong [b]

[a] The National Laboratory of Biomacromolecules, Institute of Biophysics, Chinese Academy of Sciences, Beijing 100101, China
[b] Institute of Chemistry, Chinese Academy of Sciences, Beijing 100080, China
[c] The Graduate School of Chinese Academy of Sciences, Beijing, China

Received 3 March 2005
Available online 5 April 2005

Abstract

We have attempted direct observation of the light-driven rotation of a FoF_1-ATP motor. The FoF_1-ATP motor was co-reconstituted by the deletion-δ subunit of FoF_1-ATP synthase with bacteriorhodopsins (BRs) into a liposome. The BR converts radiation energy into electrochemical gradient of proton to drive the FoF_1-ATP motor. Therefore, the light-driven rotation of FoF_1-ATP motor has been directly observed by a fluorescence microscopy using a fluorescent actin filament connected to β-subunit as a marker of its orientation. The rotational torque value of the Fo motor was calculated as 27.93 ± 1.88 pN nm. The ATP motor is expected to be a promising rotary molecular motor in the development of nanodevices.
Published by Elsevier Inc.

Keywords: FoF_1-ATPase; Rotary torque; Molecular motor; Light-driven; Proton motive force

The development of nanotechnology has enabled the design and production of a variety of nanodevices and molecular machines. The study of molecular motors that have the potential to power these nanodevices has been attracting increasing interest [1]. Biophysical analysis of many enzymes has revealed their roles as nano-motors, such as kinesin dynein, myosin, DNA helicase, and RNA polymerase as linear stepped motors, but the rotary motor was only flagella motor and ATP synthase [2]. The force generation and size scale of these biomolecular motors are compatible with nanofabricated structures. Although, many researchers have studied the ATP motor with only F_1 sub-complexes, and the subunit γ rotation during ATP hydrolysis has been demonstrated by fluorescent microscopy using a fluorescent actin filament connected to γ as a marker of its orientation [3], we know relatively little about Fo-ATP motor. Recently, the rotation of the central γ-subunit during proton-powered ATP synthesis of FoF_1-ATPase is demonstrated by the polarization detection of a single dye molecule labeled [4] and by single-molecule FRET imaging of dual labeled γ and b_2 [5]. However, both methods have the limitations such as short rotation time (several hundred milliseconds) and observation in an indirect way. So it is necessary to develop a vivid model to study the light-driven rotation of the ATP motor, not only for the biochemistry, but also for the development of nanotechnology.

ATP synthase, also named FoF_1-ATPase, is one of at least eight subunit types (α_3, β_3, δ, a, b_2, ε, γ, and c_n) which combine into two distinct regions of Fo and F_1. Fo is an ion-driven rotary engine, which can be used to function as anion pump. F_1 is a hydrolysis-driven engine which can be used to synthesize ATP from ADP and phosphor [6]. It is known that the δ-subunit plays a switch role between the Fo and F_1 in the ATP synthesis [7]. Furthermore, from the schematic of the geometric organization of FoF_1-ATP motor, one draws attention to the fact that there are two 'stalks' (ε, γ,

☆ *Abbreviations:* DCCD, *N*,*N*′-dicyclohexylcarbodiimide; CCCP, carbonyl cyanide *m*-chlorophenyl hydrazone.

* Corresponding author.
E-mail address: yuejc@sun5.ibp.ac.cn (Y. Jiachang).

0006-291X/$ - see front matter. Published by Elsevier Inc.
doi:10.1016/j.bbrc.2005.03.172

and $b_2\delta$) connecting Fo to F_1. The δ-subunit is attached to an α-subunit in F_1 and another segment connected to the b_2 subunit of Fo with the b_2 co-consisting of a 'stalk' in the peripheral FoF_1-ATPase. If the δ-subunit is deleted, only one center 'stalk' (ε, γ) is present in the FoF_1-ATP motor that is suitable for the development of nanotechnology to design and produce a new nanomotor. For this purpose, in the previous paper [8], we had developed a new model using hybrid δ-free FoF_1-ATPase of chromatophore, to image the clockwise rotation of the ATP motor. Here, we further developed this new vivid model using the FoF_1-ATP synthase and bacteriorhodopsins (BRs) co-reconstituted into a liposome. An artificial δ-free FoF_1-ATP motor was constructed with α_3, β_3, ε, γ, and c_n subunits as rotator and a, b_2 as stator. The BR converts radiation energy into electrochemical gradient of proton to drive the FoF_1-ATP motor. Using a fluorescent actin filament attached to the β-subunit, the light-driven rotation of FoF_1-ATP motor was observed directly, viewed from Fo to F_1 side under a fluorescent microscope.

Materials and methods

Reagents. Streptavidin was purchased from Sigma. Maleimido-C3-NTA and Biotin-AC5 Sulfo-OSu were purchased from Dojindo (Japan). 1,2-Dipalmitoyl-*sn*-glycero-3 phosphoethanolamine-*N*-biotinyl was from Avanti. The purified bacteriorhodopsin was kindly provided by Dr. Zhong Sheng (Institute of Biophysics, Chinese Academy of Sciences).

Preparation of fluorescent actin filaments. The G-actin was co-labeled with FITC and Maleimido-C3-NTA–Ni^{2+} in buffer (50 mM Hepes–KOH, pH 7.6, 4 mM $MgCl_2$, and 0.2 mM ATP) overnight at 4 °C. The free FITC and Maleimido-C3-NTA (Ni–NTA) were removed by a desalting column. Then the labeled G-actin was polymerized in buffer containing 50 mmol/L Hepes–KOH (pH 7.6), 50 mmol/L KCl, 4 mmol/L $MgCl_2$, and 2 mmol/L ATP.

Preparation for immobilization of proteoliposomes in the experimental system for observation. Biotin-AC5-Sulfo-OSu was linked to the polylysine which had previously coated on the bottom of the dishes, and then 100 μl of 10 nM streptavidin was added onto the dish bottom. After 5 min, the free streptavidin was washed. The proteoliposomes were conjugated by lipid–biotin–streptavidin–biotin–polylysine to the glass surface. And then the FITC-labeled F-actin filaments were attached to the β-subunit of F_1 part through the His-tag with Maleimido-C3-NTA, as a marker of orientation for observation under an Olympus IX71 fluorescent microscope equipped with an ICCD camera.

Purification of the β-subunit, F_1 ($\alpha_3\beta_{(10\times\text{his-tag})3}\gamma$), and $FoF_{1\text{-ATPase}}$. The F_1-ATPase coding sequence was isolated from thermophilic bacterium PS3, and site-directed mutations of a cys193ser and gamaser107cys were introduced and a 10 *histidine* tag was inserted downstream of the initiation codon, the mutated construct, pGEM-MH, was then cloned into the expression plasmid pQE-30,and the expression plasmid pQE-MH was inserted into *Escherichia coli* JM103(*uncB-UncD*) in which a majority of F_1-ATPase genes have been eliminated. Thermophilic bacterium, *Bacillus* PS3$\beta_{10\times\text{his-tag}}$ subunit ($TF_1\beta$), and F_1-ATPase ($\alpha_3\beta_{(10\times\text{his-tag})3}\gamma$) were expressed and purified as in [9], in which the JM103 strain expressing F_1-ATPase was cultured in 2× YT medium (AMP^+) for 3–4 h at 37 °C. When the A_{660} was increased to 0.6–0.8, the expression of the F_1-ATPase was induced by addition of 1 mmol/L isopropylthio-β-D-galactoside for 3 h. Cells were harvested by centrifuging for 15 min at 4000*g* and cell extracts were prepared using lysozyme (1 mg/mL)/sonication (5 min) in 50 mmol/L Tris–HCl (pH 8.0) buffer containing 0.5 mol/L NaCl and 1 mmol/L phenylmethane sulfonyl fluoride. The extracts were incubated at 60 °C for 30 min, and $TF_1\beta$ was purified using Ni^{2+}–NTA affinity chromatography at 4 °C. F_1-ATPase ($\alpha_3\beta_{(10\times\text{his-tag})3}\gamma$) was purified as described in [10] at 25 °C. The FoF_1-ATP synthase also from the *E. coli* JM103(*uncB-UncD*) was purified as described by Foster [9]. The mutant ATP synthase containing the His-tag could be isolated with Ni–NTA column. FoF_1-ATPase was eluted with buffer B containing 0.05% lysolecithin and 250 mM imidazole at 4 °C, and then further purified by a gel filtration column (Superdex 200 HR 10/30 Pharmacia). The purified protein was analyzed by SDS–PAGE.

Results and discussion

FoF_1-ATPase from the *E. coli* JM103(*uncB-UncD*) was purified as [9]. The purified BR and FoF_1-ATPase were co-reconstituted into a liposome. The liposome was prepared by reverse-phase evaporation with the mixture of soybean lipid and 1,2-dipalmitoyl-*sn*-glycero-3 phosphoethanolamine-*N*-biotinyl (molar ratio: 7:0.001) [11]. The molar ratio of BR and FoF_1-ATPase was about 100:1, and that of lipids and protein was 30:1(w/w). This is able to gain about one FoF_1-ATPase and more than 20 BR molecules in one proteoliposome.

The procedure of the deletion δ-subunit of FoF_1-ATPase is briefly shown in Figs. 1A–D. The proteoliposome containing FoF_1-ATPase and BR was incubated in the buffer with 2 M LiCl, 0.1 mM Tricine–NaOH, 10 mM $MgCl_2$, and 1 mM ATP for 20 min at 4 °C. Then the proteoliposome was washed with the buffer and isolated by centrifuging. As the treatment of FoF_1-ATPase with LiCl removed not only β subunits but also some α and δ subunits, the LiCl-treated proteoliposome was co-incubated with purified $\alpha_3\beta_3\gamma$ (or β) subunit at 4 °C for 60 min (for each divided subunit of F_1-ATP with buffer 0.1 mM Tricine–NaOH, 10 mM $MgCl_2$, 50 mM KCl, 0.5 mol/L NaCl, and 1 mM ATP), and then further incubated 37 °C for 60 min (for reconstituted δ-free FoF_1-ATPase). The proteoliposome was further isolated to obtain the reconstituted δ-free FoF_1-ATPase.

The ATP hydrolysis/synthesis activity assay was used to evaluate the reconstituted FoF_1-ATPase [12]. As shown in Table 1, before the LiCl treatment, FoF_1-ATPase in the proteoliposome had a good ATP hydrolysis/synthesis activity. Most of ATP hydrolysis/synthesis activity was lost in the LiCl-treated FoF_1-ATP synthase. After incubation with $F_1(\alpha_3\beta_{(10\times\text{his-tag})3}\gamma)$, 53% of its hydrolysis activity was restored. However, the ATP synthesis activity of the δ-less proteoliposome was only restored to about 6%, which was much lower than that of the ATP hydrolysis activity (53%). If only the purified β-subunit was used instead of $F_1(\alpha_3\beta_{(10\times\text{his-tag})3}\gamma)$, the ATP hydrolysis activity was restored by about 5%. These

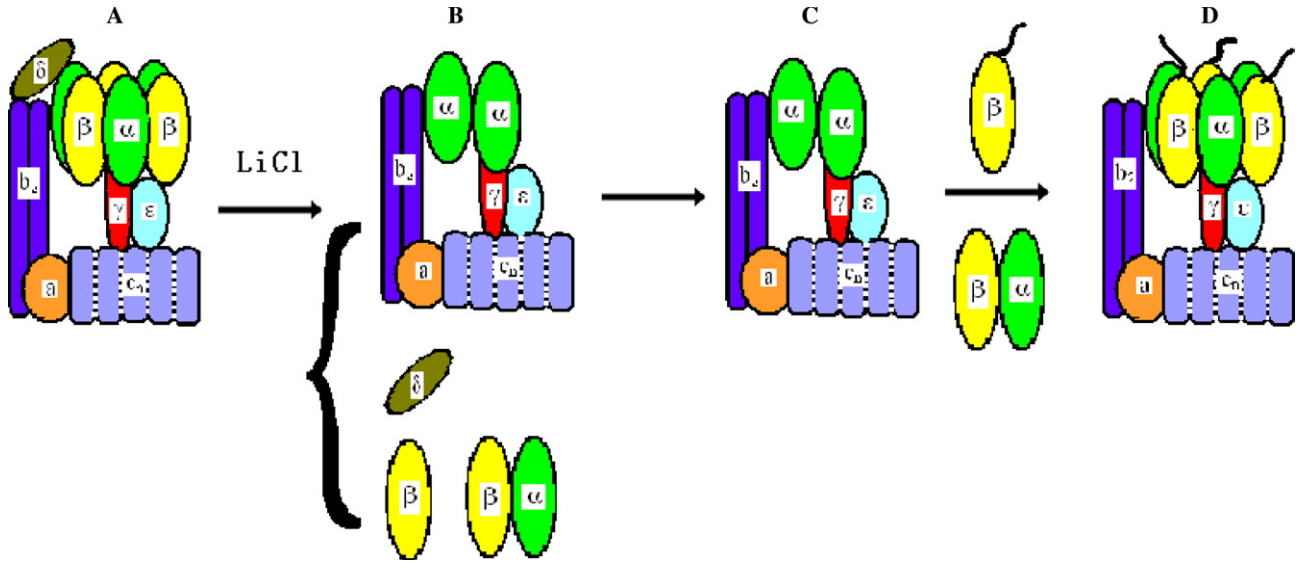

Fig. 1. The procedure of the reconstitution of δ-free F_1-ATP motor. (A) The FoF_1-ATPase; (B) the FoF_1-ATPase with LiCl-treatment; (C) rebinding purified β,α-subunit; and (D) the reconstituted δ-deleted FoF_1.

Table 1
The ATP hydrolysis/synthesis activity restored in reconstituted δ-less FoF_1-ATPase

	Purified β[a] (%)	$F(\alpha_3\beta_{(10\times\text{his-tag})3}\gamma)$[b] (%)	Reconstituted FoF_1-ATPase (%)
ATP hydrolysis activity restored	5	53	100
ATP synthesis activity restored	No	6	100

[a] Five micrograms of LiCl-treated FoF_1-ATPase and 50 μg purified β was reconstituted.
[b] Five micrograms of LiCl-treated FoF_1-ATPase and 50 μg $F_1(\alpha_3\beta_{(10\times\text{his-tag})3}\gamma)$ was reconstituted.

results indicated that β subunits were removed from FoF_1-ATPase together with some α and δ subunits with the LiCl-treatment. After the incubation of $F_1(\alpha_3\beta_{(10\times\text{his-tag})3}\gamma)$ with the LiCl-treatment of FoF_1-ATPase, some of FoF_1-ATPase were reconstituted with β- and α-subunits to be only δ-free. The FoF_1-ATPase was used as the new ATP motor model for the clockwise rotation. The FoF_1-ATPase could be stored at −70 °C with 20% glycerol for 3 months before using.

The imaging of the FoF_1-ATP motor rotation is shown in Fig. 2. A FITC-labeled actin filament was attached to the β-his-tag subunit in the proteoliposome, which was immobilized onto the glass surface through the biotin–streptavidin–biotin coupling. The sample was exposed

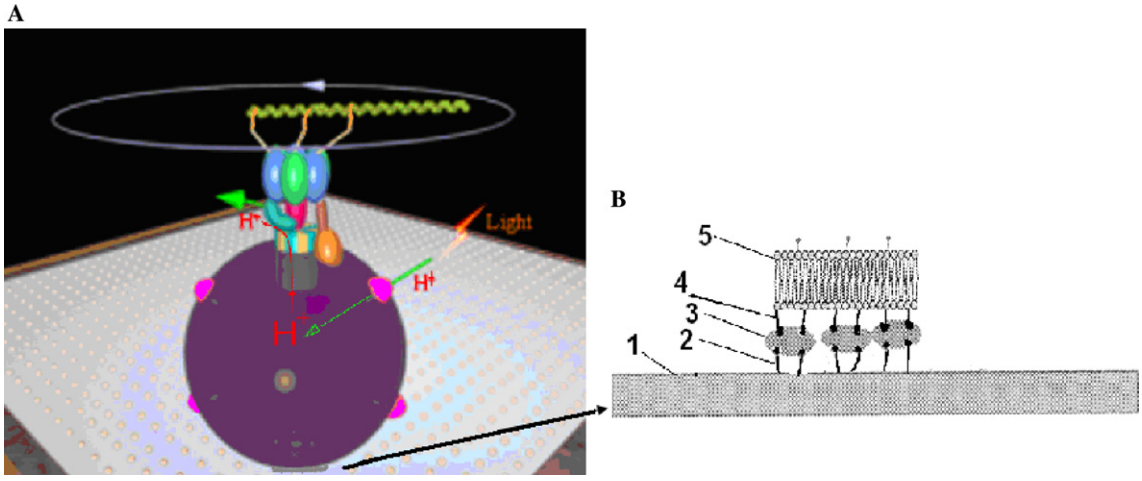

Fig. 2. The schematic of the light-driven FoF_1-ATP motor. (A) The schematic of FoF_1-ATP motor; (B) the schematic of FoF_1-ATP motor was immobilized on the surface of glass. The cover glass in a chamber through the biotin–streptavidin–biotin coupling. (1) The cover glass; (2) biotin-AC5 Sulfo-OSu; (3) streptavidin; (4) phosphoethanolamine-*N*-biotinyl; and (5) the proteoliposome.

under the cooled light source with a 570 nm filter for 30 min to initiate the rotation of the FoF_1-ATP motor. Before illumination, the buffer containing 2 mM NaN_3 and 2 mM ATP was infused into the chamber, the clockwise rotation of *actin* filament was observed directly in an Olympus IX71 fluorescent microscope equipped with an ICCD camera (Roper Scientific, Pentamax EEV 512 × 512 FT). Fig. 3 shows an example of the sequential images of a rotary fluorescent actin filament attached to FoF_1-ATP motor with 100 ms time interval between each image. It is clear that the rotational orientation is clockwise viewed from the Fo side to F_1. If NaN_3/ATP were not used in the buffer, no rotary filament was found. The addition of NaN_3/ATP to the proteoliposomes not only inhibited the hydrolysis activity of the FoF_1-ATPase, but also helped to hold force between the β_3 and γ to tightly band them together [13]. Therefore, the rotary fluorescent actin filament attached to the β-subunit of F_1 was clockwise observed directly from the Fo side to F_1.

Worthy of mention is that in our experiment, the rotation event of FoF_1-ATP motor was rare. On an average about 1/200 filaments started to rotate after illumination while others were immobile on the glass surface. Although the proteoliposome was fixed to the glass surface through the lipid–biotin–streptavidin–biotin–polylysine coating bottom of the dishes, some of the filaments were still torn off near the attachment point and floated into solution (about 1/300). We have found more than 20 rotary filaments connected to FoF_1-ATP motor and the rotation of six filaments with different lengths is shown in Fig. 4. It can be seen that the rotary rates of many filaments were not constant with some of them having occasional pause and imaged even backwards. This phenomenon may be caused by the frictional role of the protein same as that in F_1-motor imaging [14].

Several control experiments were performed to confirm that the rotation of the ATP motor is regulated by electrochemical gradient of proton. As shown in Fig. 5, Fig. 5A is the rotating filament stopped immediately when 5 μl of 10 μM CCCP was added (arrowhead the curve). It was also found that if the sample is in dark or incubation with DCCD before the illumination, no rotary filament is observed (data are not shown). The reason is that CCCP destroyed the proton driven force

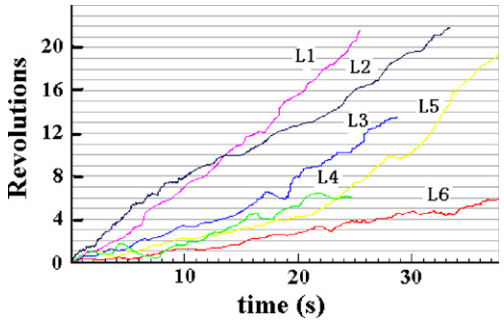

Fig. 4. Examples of time courses of the rotation of the fluorescent actin filaments attached to the $\beta_{10\times his\text{-}tag}$ of FoF_1-ATP motor. The lengths of the filaments, L1, L2, . . . , L6, are, 1.7, 1.9, 2.0, 2.3, 2.8, and 3.3 μm, respectively.

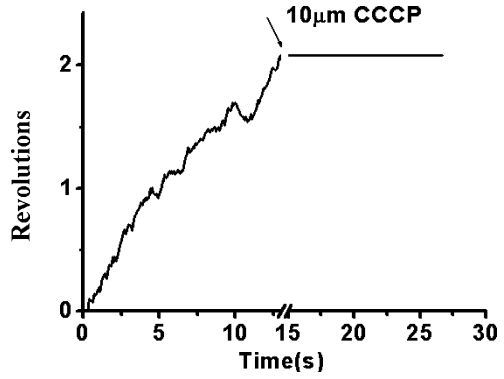

Fig. 5. The rotating filament was stopped by adding CCCP.

and DCCD was an inhibitor of Fo channel. These results demonstrated that the rotation of filaments depended on the proton driven force produced in Fo. It is interesting that the proteoliposomes can be keeping up the electrochemical gradient of protons for a long time. After the illumination, some filaments rotated continuously for more than 20 min. This phenomenon could be explain as the following two reasons: First, in our experiment, many proteoliposomes consisted of one FoF_1 motor and a lot of BR molecules converting radiation energy to generate protons; Second, the proteoliposome seems to be a reservoir to store the energy that was converted by BR and the proton-driven motor rotary in Fo c-ring was like a strobe of the reservoir to

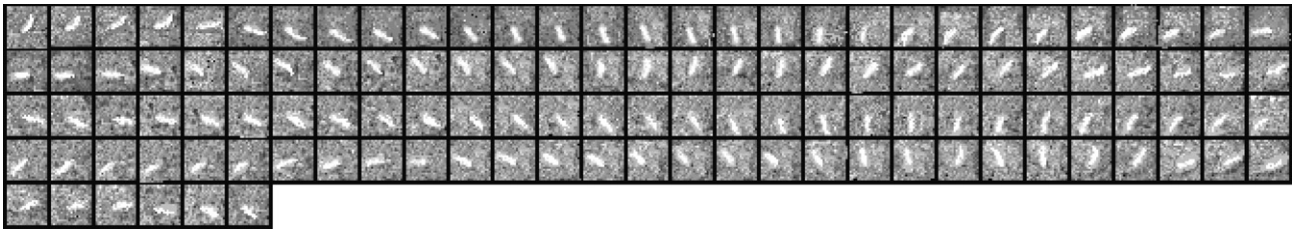

Fig. 3. The sequential images of a rotating fluorescent actin filament (L6). The clockwise rotation of the fluorescent actin filaments attached to the $\beta_{10\times his\text{-}tag}$ of FoF_1-ATPase was observed with experimental system. Time interval between images was 100 ms, the rotational orientation was clockwise viewed from the Fo side to F_1.

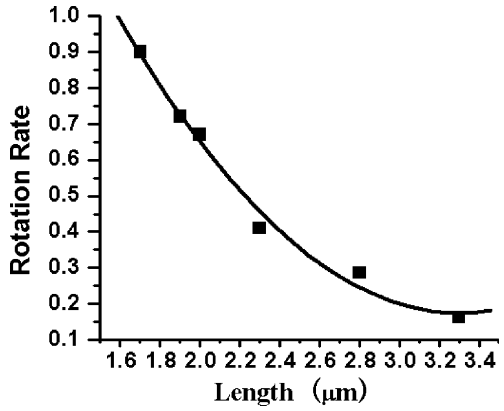

Fig. 6. The relationships between the rotating speed and the length of fluorescent actin filaments. The lengths of fluorescent actin filaments, L1, L2, ..., L6, are 1.7, 1.9, 2.0, 2.3, 2.8, and 3.3 μm respectively, The rotary ratio: 0.9, 0.72, 0.67, 0.41, 0.286, and 0.162, (R.P.S.), respectively.

release protons, and also coupled a stalk (ε, γ) of F_1 to carry out rotation of the $\alpha_3\beta_3$ hexamer with high load, but not ATP synthesis.

We further characterized the rotation speed of the ATP motor. As shown in Fig. 6, the rotation speed decreased with the length of filaments ranging from 1.7 to 3.3 μm. This indicated that the rotation speed of motor depended on the F_1 load. The frictional torque of the rotation is calculated by the equation developed by: $(4n\pi^2/3)\ \eta L^3/[\ln(L/2r) - 0.447]$, where n is the rotary rate, $\eta(10^{-3}\ \mathrm{N\ s\ m^{-2}})$ is the viscosity of the medium, L is the length of actin filament, and r (5 nm) is the radius of filament [14]. The averaged frictional torque calculated from the six actin filaments in Fig. 6 is 27.93 ± 1.88 pN nm. It has been reported that the rotary torque stalls a load of about 40 pN in the ATP hydrolysis driven in F_1, and about 24 pN of proton driven in Fo [15,16]. The rotary torque produced in our experiment was closed to this one.

A new δ-free FoF_1-ATP motor was constructed in the proteoliposome to provide a feasible model to study the clockwise rotation of the ATP motor. Using this model, we have directly observed the rotary torque produced by Fo c-ring rotation of a FoF_1 motor. The light-driven rotation of the motor has been successfully observed for a certain period of time. The further optimization and development of the proteoliposomes system is underway to make it an important model for the investigation of the coupling of Fo to F_1-ATP motor and a useful biomolecular motor in nanotechnology.

Acknowledgments

We thank Prof. Yang Fuyu (The National Laboratory of Biomacromolecules, Institute of Biophysics, Chinese Academy of Sciences), for helpful discussion and encouragements and thank Prof. Zhou Junmei for her reading the manuscript. We also thank Prof. Montemagno C. (UCLA, USA) who kindly provided the Engineered F_1-ATPase. Grant to this work was provided by Programs of National Natural Science Foundation of China (Nos. 30292905, 90306005).

References

[1] G.D. Bachand, R.K. Soong, H.P. Neves, A. Qlkhovets, H.G. Graighoad, G.D. Montemagno, Precision attachment of individual F1-ATPase biomolecular motors on nanofabricated substrates, Nano Lett. 1 (2001) 42–44.
[2] H. Noji, R. Yasuda, M. Yoshida, K. Kinosita Jr., Direct observation of the rotation of F1-ATPase, Nature 386 (1997) 299–302.
[3] A. Kaim, M. Drummer, B. Sick, Lo. Zumofer, A. Renn, U. Wild, P. Dimroth, Coupled rotation within single FoF1 enzyme complexes during ATP synthesis or hydrolysis, FEBS Lett. 525 (2002) 1560163.
[4] M. Diez, B. Zimmermann, M. Borsch, M. Konig, E. Schweinberger, S. Steigmiller, S. Felekyan, V. Kudryavtsev, C.A.M. Seidel, P. Graber, Proton powered subunit rotation in single membrane-bound F0F1-ATP syntheses, Nat. Struct. Mol. Biol. 11 (2004) 135–141.
[5] P.D. Boyer, The binding change mechanism of ATP syntheses—some probabilities and possibilities, Biochem. Biophys. Acta 1140 (1993) 215–250.
[6] J. Weber, M.S. Wilke, A.E. Senior, Proton-powered subunit rotation in single membrane-bound F0F1-ATP synthase possibilities, J. Biol. Chem. 277 (2002) 18390–18396.
[7] Y.B. Cui, Y.H. Zhang, J.C. Yue, P.D. Jiang, Direct observation of the clockwise light-driven rotation of F0F1-ATP synthase complex, Chin. Sci. Bull. 13 (49) (2004) 1342–1347.
[8] M. Yoshinori, I. Atsuko, H. Hironri, M. Masatomo, M. Futai, One-step purification of *Escherichia coli* H^+-ATPase(F_0F_1) and its reconstitution into liposomes with neurotransmitter transporters, J. Biol. Chem. 266 (1991) 22141–22146.
[9] E.J. Gordon, L.E. Strong, L.L. Kiessling, Q. Yang, X.Y. Liu, J. Miyake, H. Toyotama, Self-assembly and immobilization of liposomes in fused-silica capillary by avidin–biotin binding, Supramol. Sci. 5 (1998) 769–772.
[10] C. Montemagno, G. Bachand, Constructing biological motor powered nanomechanical devices, Nanotechnology 10 (1999) 225–231.
[11] T. Matsui, M. Yoshida, The induction kinetics of bacterial photophosphorylation threshold effects by the phosphate potential and correlation with the amplitude of the carotenoid absorption band shift, Biochema. Biophys. Acta 1231 (1995) 139–146.
[12] Y. Zhou, M.D. Thomas, R.L. Cross, Subunit rotation in *Escherichia coli* FoF_1-ATP synthase during oxidative phosphorylation, Proc. Natl. Acad. Sci. USA 94 (1997) 10583–10587.
[13] E. Muneyuki, M. Makino, H. Kamata, Y. Kagawa, M. Yoshida, H. Hirata, Inhibitory effect of NaN_3 on the F_0F_1 ATPase of submitochondrial particles as related to nucleotide binding, Biochim. Biophys. Acta 16 (1144) (1993) 62–68.
[14] R. Yasuda, H. Noji, M. Yoshida, K. Kinosita Jr., H. Itoh, Resolution of distinct rotational substeps by submillisecond kinetic analysis of F1-ATPase, Nature 410 (2001) 898–904.
[15] W. Junge, ATP synthase and other motor proteins, Proc. Natl. Acad. Sci. USA 96 (1999) 4735–4737.
[16] R. Berry, The molecular motors, in: Manfrod Schliwa (Ed.), The Bacterial Flagellar Motor, 2003, 120 pp.